

STUDY OF DELAYED CRACKING BEHAVIORS OF  
HYDROGEN-CHARGED SUS304L DEEP DRAWN  
CYLINDRICAL CUPS UNDER ELEVATED BLANK HOLDING  
FORCES

MOHD SHAHIR BIN HADZIR

FACULTY OF ENGINEERING  
UNIVERSITY OF MALAYA  
KUALA LUMPUR

2022

**STUDY OF DELAYED CRACKING BEHAVIORS OF  
HYDROGEN-CHARGED SUS304L DEEP DRAWN  
CYLINDRICAL CUPS UNDER ELEVATED BLANK  
HOLDING FORCES**

**MOHD SHAHIR BIN HADZIR**

**RESEARCH PROJECT SUBMITTED IN PARTIAL  
FULFILMENT OF THE REQUIREMENTS FOR THE  
DEGREE OF MASTER OF MECHANICAL  
ENGINEERING**

**FACULTY OF ENGINEERING  
UNIVERSITY OF MALAYA  
KUALA LUMPUR**

**2022**

**UNIVERSITY OF MALAYA**  
**ORIGINAL LITERARY WORK DECLARATION**

Name of Candidate: MOHD SHAHIR HADZIR

Matric No: S2021322

Name of Degree: Master of Mechanical Engineering

Title of Project Paper/Research Report/Dissertation/Thesis (“this Work”):

Study of Delayed Cracking behaviors of Hydrogen-Charged SUS304L Deep  
Drawn Cylindrical Cups Under Elevated Blank Holding Forces

Field of Study: Mechanical Engineering (Material Processing Technology , Metal  
Forming)

I do solemnly and sincerely declare that:

- (1) I am the sole author/writer of this Work;
- (2) This Work is original;
- (3) Any use of any work in which copyright exists was done by way of fair dealing and for permitted purposes and any excerpt or extract from, or reference to or reproduction of any copyright work has been disclosed expressly and sufficiently and the title of the Work and its authorship have been acknowledged in this Work;
- (4) I do not have any actual knowledge nor do I ought reasonably to know that the making of this work constitutes an infringement of any copyright work;
- (5) I hereby assign all and every rights in the copyright to this Work to the University of Malaya (“UM”), who henceforth shall be owner of the copyright in this Work and that any reproduction or use in any form or by any means whatsoever is prohibited without the written consent of UM having been first had and obtained;
- (6) I am fully aware that if in the course of making this Work I have infringed any copyright whether intentionally or otherwise, I may be subject to legal action or any other action as may be determined by UM.

Candidate’s Signature

Date: 10/3/2022

Subscribed and solemnly declared before,

Witness’s Signature

Date: 10/3/2022

Name:

Designation:

**STUDY OF DELAYED CRACKING BEHAVIORS OF HYDROGEN-  
CHARGED SUS304L DEEP DRAWN CYLINDRICAL CUPS UNDER  
ELEVATED BLANK HOLDING FORCES**

**ABSTRACT**

In this paper the effect of hydrogen charged SUS304L deep drawn cylindrical cups under elevated blank holding forces are investigated. A round SUS 304L blanks was deep drawn at 8, 9, 10 and 11 kN blank holding force, BHF using a die, after the specimens were hydrogen charged for 6, 12, and 24 hours in 1N of H<sub>2</sub>SO<sub>4</sub> and As<sub>2</sub>O<sub>3</sub> solution. It was found that the hydrogen charging of deep drawn cups has resulted in an accelerated appearance of the delayed cracks on the SUS 304L blanks. The 6 hours charged specimen was also deep drawn again using TiN coated die at 7, 10 and 12 kN of BHF, and it was found that delayed cracks still occur, but did not develop as fast as using uncoated die. Understanding the effect blank holding force with hydrogen towards the SUS304L will allow better understanding of the steel characteristic for future application.

Keywords: Hydrogen Charging, Blank Holding Force (BHF), Stainless Steel SUS 304L, Delayed Crack

**KAJIAN TINGKAH LAKU KERETAK YANG TERTANGGUH SUS304L  
CAWAN SILINDER PENAIKAN DALAM BERCAS HIDROGEN DI BAWAH  
DAYA TAHAN KOSONG YANG DITINGKATKAN**

**ABSTRAK**

Di dalam kertas kerja ini, kesan cawan silinder penaikan dalam SUS304L bercas hidrogen di bawah daya pegangan kepingan yang dinaikkan telah disiasat. Kepingan bulat SUS 304L telah ditekan pada daya penahan kosong 8, 9, 10 dan 11 kN, BHF menggunakan acuan, selepas spesimen dicas oleh hidrogen selama 6, 12, dan 24 jam dalam 1N larutan H<sub>2</sub>SO<sub>4</sub> dan As<sub>2</sub>O<sub>3</sub>. Didapati bahawa pengecasan hidrogen bagi cawan penaikan dalam telah menyebabkan kemunculan keretakan tertunda pada kepingan SUS 304L semakin pantas. Spesimen yang dicas selama 6 jam juga di lakukan penanikan dalam sekali lagi menggunakan acuan bersalut TiN pada 7 , 10 dan 12 kN BHF, dan didapati retakan tertangguh masih berlaku, tetapi tidak berkembang secepat menggunakan acuan tidak bersalut. Memahami kesan daya pegangan kosong dengan hidrogen terhadap SUS304L akan membolehkan pemahaman yang lebih baik tentang ciri keluli untuk aplikasi masa hadapan.

Kata kunci: Pengecasan Hidrogen , Daya Tahan Kepingan (BHF), Keluli Tahan Karat SUS 304L, Retak Tertunda

## ACKNOWLEDGEMENTS

First and foremost, I would like to praise and thank the almighty God for providing me the strength and endurance to finish this dissertation entitled “Study of Delayed Cracking behaviors of Hydrogen Charged SUS304L Deep Drawn Cylindrical Cups Under Elevated Blank Holding Forces”.

My highest gratitude goes to my supervisor Ir Dr Tan Chin Joo for his vast guidance and knowledge that tirelessly guides me towards the completion of this project & dissertation. My gratitude also extends to my friends that is always there to support me during the toughest time.

Finally, to my parents & sisters, I would like to express my special heartfelt gratitude for their unrelentless & continuous support in supporting me throughout this journey until the end.

Universiti Malaysia

## TABLE OF CONTENTS

<b>Abstract</b> .....	<b>iii</b>
<b>Abstrak</b> .....	<b>iv</b>
<b>Acknowledgements</b> .....	<b>v</b>
<b>Table of Contents</b> .....	<b>vi</b>
<b>List of Figures</b> .....	<b>viii</b>
<b>List of Tables</b> .....	<b>x</b>
<b>List of Symbols and Abbreviations</b> .....	<b>xi</b>
<b>CHAPTER 1: INTRODUCTION</b> .....	<b>13</b>
1.1 Background of Study .....	13
1.2 Problem Statement.....	15
1.3 Objectives of study .....	15
1.4 Scope of Study.....	16
<b>CHAPTER 2: LITERATURE REVIEW</b> .....	<b>17</b>
2.1 Stainless Steel Material.....	17
2.2 Hydrogen Charging .....	17
2.2.1 Introduction of hydrogen by cathode .....	18
2.3 Hydrogen Embrittlement .....	19
2.4 Hydrogen diffusion and solubility .....	19
2.4.1 Microstructural influence .....	20
2.5 Delayed Cracking .....	21
2.6 Effect of residual stress.....	22
<b>CHAPTER 3: METHODOLOGY</b> .....	<b>25</b>

3.1	Introduction.....	25
3.2	Experimental Flow Chart.....	26
3.3	Preparation of electrolytic & arsenic solution .....	27
3.4	Hydrogen charging .....	27
3.5	Deep Drawing.....	28
<b>CHAPTER 4: RESULTS &amp; DISCUSSION.....</b>		<b>31</b>
4.1	Hydrogen Charging .....	31
4.2	Deep drawing at elevated BHF.....	32
<b>CHAPTER 5: CONCLUSION.....</b>		<b>39</b>
5.1	Summary.....	39
5.2	Recommendations for Future Project.....	39
<b>REFERENCES.....</b>		<b>41</b>

## LIST OF FIGURES

Figure 2.1 : (a) Effect of hydrogen charging periods on the hydrogen content of the 304 stainless steels (b) Effect of hydrogen charging times on the Vickers hardness of the 304 stainless steels (c) Effect of hydrogen charging times on the absorbed impact energy of the 304 stainless steels (Sang P.L, et. al, 2015) .....	18
Figure 2.2 : Schematic illustration of hydrogen diffusion path (a) from surface and (b) near crack tip. The transformed martensite acts as a highway for hydrogen diffusion in surrounding austenites (T. Kanazaki et. al, 2008).....	19
Figure 2.3 : Tangential residual stresses in $\alpha'$ -martensite and austenite, Papula.S , et al (2015),.....	21
Figure 2.4 : Hoop stress distribution at inner and outer surfaces of the cup at end of drawing stages (a) and tool separation stages (b) (Tan & Aslian , 2019) .....	23
Figure 3.1 : Experimental flow chart .....	26
Figure 3.2 : Setup for the hydrogen charging of the SUS 304L blanks .....	28
Figure 3.3 : (a) TiN Coated Die (b) Uncoated Die (Tan CJ et. al 2019).....	29
Figure 3.4 : Surface roughness profile of TiN coated die (Tan CJ et. al 2019) .....	29
Figure 3.5 : Surface roughness profile of finely polished SKD-11 tool steel uncoated die (Tan CJ et. al 2019).....	29
Figure 3.6 : Setup for the Deep drawing process for blank holding force BHF (Tan CJ et. al 2019).....	30
Figure 4.1 : Non hydrogen charged blanks (left), Hydrogen charged blanks (right).....	31
Figure 4.2 : Hydrogen charged SUS304L cup (left) Non hydrogen charged cups (right) .....	32
Figure 4.3 : Samples charged for 24 hours after deep drawn.....	32
Figure 4.4 : Number of cracks comparison for HC sample before BHF and vice versa	33
Figure 4.5 : Crack length comparison for HC sample before BHF and HC after BHF	34
Figure 4.6 : Crack length comparison for HC sample before BHF and HC after BHF ..	34
Figure 4.7 : Peak Forming Load vs HC duration.....	37

Figure 4.8 : Maximum drawing load comparison between HC after deep drawing samples and HC before deep drawing.....37

Figure 4.9 : Forming load vs punch stroke for TiN Coated die samples hydrogen charged for 6 hours .....38

Figure 4.10 : Forming load vs punch stroke for un-coated die HC after deep drawing..38

Figure 4.11 : Forming load vs Punch stroke for un-coated die HC before deep drawing .....38

Universiti Malaya

## LIST OF TABLES

Table 3-1 : Chemical composition of SUS 304L blanks.....	25
Table 3-2 : Chemical composition of SUS 304 blanks .....	25
Table 4-1 : Number of crack and crack lengths for HC after BHF, (HCAB), HC before BHF, (HCBB) and HC before BHF with TiN die, (HCBB-TiN) samples .....	35

Universiti Malaya

## LIST OF SYMBOLS AND ABBREVIATIONS

H <sub>2</sub> SO <sub>4</sub>	:	Sulphuric Acid
As <sub>2</sub> O <sub>3</sub>	:	Arsenic (III) Oxide
SiO <sub>2</sub>	:	Silicon Dioxide
SUS304L	:	(Steel Use Stainless) Stainless Steel 304L in Japanese JIS Standard
mA/cm <sup>2</sup>	:	Current density, milliamp per centimeter squared
M	:	Molarity
N	:	Normality
ppm	:	Part per million
Pt	:	Platinum
Hv	:	Vickers Hardness
C	:	Carbon
S	:	Sulphur
P	:	Phosphorus
Mn	:	Manganese
Si	:	Silicon
Cr	:	Chromium
Ni	:	Nickel
N	:	Nitrogen
kN	:	Kilo newton

## CHAPTER 1: INTRODUCTION

### 1.1 Background of Study

A nickel / chromium stainless steel (Cr-Ni, approximately 18% Cr, 8% Ni) possesses good corrosion resistance, versatile shape / forming capability & welding properties. In recent years, the rise of hydrogen energy as a candidate for zero emission energy has raised the need for better transportation of hydrogen gas. As a high performing material such as stainless steel, SUS304L has is deemed as one of the promising candidates for hydrogen fuel cell (FC) storage tanks. Due to their great resistance to hydrogen and low temperature embrittlement, stable austenitic Cr–Ni steels are commonly employed nowadays.

However, the formation of hydrogen embrittlement or delayed cracks due to the deformation-induced martensite has permits & limited its application & performance. In austenitic stainless steels, hydrogen embrittlement is hydrogen diffusion that is highly impacted by martensitic transformation and is unhindered by strain in the absence of martensitic transformation. (T. Kanezaki, et al. 2008). Delayed cracks occurs when a steel component with previously created flaws is charged with hydrogen and subjected to a sub-critical stress. The hydrogen may be introduced during the material processing or simply from corrosion in service condition. After procedures such as deep drawing, delayed cracking can occur in metastable austenitic stainless steels. It could take hours, days, or even weeks, for cracks to occur in well produced components. Formation of delayed cracks in deep drawing of SUS304L drawn cups formed from hydrogen-charged blanks will be investigated under normal and elevated blank holding forces.

In addition, Benson et al. (1968), also reported that due to martensitic transformation, austenitic stainless steels with lower austenitic stability were more susceptible to hydrogen embrittlement than stainless steels with higher austenitic stability. Thus, to imitate the effect of hydrogen on the stainless steel, the samples will be charged & the influence of the charging durations on the time taken for the 1st appearance of the cracks in the cups formed with the two methods will be compared in this study

Universiti Malaya

## 1.2 Problem Statement

- The interaction between hydrogen and metals has been widely explored in numerous areas during the last several decades for a variety of reasons, such as the development of solid hydrogen storage systems for transportation purposes.
- Stainless steel SUS304L has potential applications for hydrogen fuel cell vehicles as storage tanks due to its high formability. It is the most common stainless steel due to its price and corrosion resistance.
- The formation of hydrogen embrittlement or delayed cracks due to the coexistence of a tiny amount of hydrogen content in the steel, the deformation-induced martensite and the tensile residual stress during the deep drawing process
- Stainless steel such as SUS304L has potential applications for hydrogen fuel cell vehicles as storage tanks. However, the formation of hydrogen embrittlement or delayed cracks due to the deformation-induced martensite has limited its application.

## 1.3 Objectives

1. To investigate the effect of hydrogen charging of the SUS304L blanks on the formation of delayed cracks in the drawn cups
2. To investigate the effect of hydrogen charging on the delayed cracking behavior of the SUS304L drawn cups formed from non-hydrogen charged blanks
3. To investigate the possibility of preventing the delayed crack due to hydrogen charging using elevated blank holding force with TiN coated die

## 1.4 Scope of Study

Delayed crack on hydrogen charged deep drawn cylindrical cups under elevated blank holding force (BHF) can be formed after a period of time after to the blanks after it is drawn into cups. Delayed cracks are attributed to the coexistence of hydrogen in the material, strain-induced  $\alpha'$ -martensite, and tensile residual stress.

The study will be carried out onto the round samples of SUS 304L blanks that has been laser cut to round shape. The samples will be separated into groups that consist of prior to BHF deep drawing samples and after BHF deep drawing samples. The BHF used is 8,9,10 and 11 kN respectively using uncoated die. Additional 3 samples will undergo BHF of 7, 10 and 12 kN using coated die to see if the delayed cracks are prevented.

Hydrogen charging will be conducted for 6, 12 and 24 hours in a 1N  $\text{H}_2\text{SO}_4 + \text{As}_2\text{O}_3$  solution. The samples are then will be observed for the duration that it is required for the delayed crack to develop over time. The effect of the hydrogen charging towards the samples were studied and investigated.

## CHAPTER 2: LITERATURE REVIEW

### 2.1 Stainless Steel Material

Stainless steel material is classified as a group of iron-base alloy Iron-Chromium, Fe-Cr alloys, that is often with an addition of Nickel, Ni. It is well known for its corrosion resistant properties such as towards salt water or acids, and also will not scale up to temperature of 1100°C. The most widely used grade of stainless steel are the austenitic Cr-Ni stainless steel, which covers almost all major production around the globe. In general, there a few types of stainless steel which is the austenitic stainless steel, ferritic stainless steel, martensitic stainless steel and duplex (combination of austenitic and ferritic stainless steel).

### 2.2 Hydrogen Charging

As reported by Sang P.L, et al (2015), austenitic stainless steel, SUS 304 hydrogen content (ppm) ranges between 6 to 11 ppm for a charging duration between 0 to 24 hour using  $H_2SO_4+As_2O_3$  & Pt wire as anode. It was also reported that the Vickers hardness increased by 1.2 times from 330 to 405 Hv due to the surface hardening cause the Hydrogen, which lead to the reduction of impact energy of the SUS304. Hydrogen embrittlement is closely associated to  $\alpha'$ -martensite transformation as  $\alpha'$ -martensite works as an effective medium for hydrogen diffusion. Due to this, the use of austenitic stainless steels like SUS301, SUS304, and SUS316 in hydrogen-containing environments is usually limited as reported by Bak, Abro, & Lee (2016).

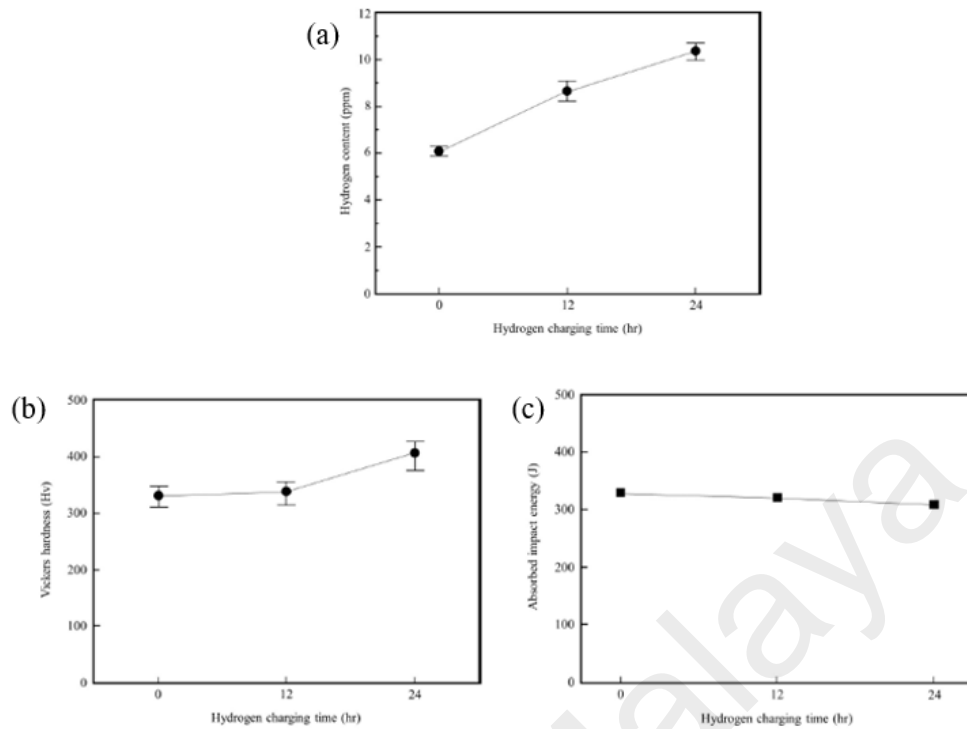


**Figure 2.1 : (a) Effect of hydrogen charging periods on the hydrogen content of the 304 stainless steels (b) Effect of hydrogen charging times on the Vickers hardness of the 304 stainless steels (c) Effect of hydrogen charging times on the absorbed impact energy of the 304 stainless steels (Sang P.L, et. al, 2015)**

### 2.2.1 Introduction of hydrogen by cathode

In an electrolyte, samples are charged. Hydrogen molecules will develop on the sample's surface (cathode) when an external current is applied. Different electrolytes, such as water, NaCl, and NaOH, can be used, but the most frequent electrolyte is H<sub>2</sub>SO<sub>4</sub> in water. Because of its size, hydrogen molecules struggle to penetrate into the samples. As a result, a hydrogen recombination poison, such as As<sub>2</sub>O<sub>3</sub>, is typically added with the electrolyte to inhibit the production of molecular gaseous hydrogen. (A.P Bentley and G.C Smith, 1986). Experiments have also revealed that as the current density and charging duration increases, so does the hydrogen content inside the sample. This approach is commonly used to investigate stainless steel embrittlement. (DeLuccia, J., 1988).

## 2.3 Hydrogen Embrittlement

Benson et al. (1968) reported that austenitic stainless steels with lower austenitic stability were more sensitive to hydrogen embrittlement than stainless steels with high austenitic stability due to martensitic transformation. Murakami .Y et. al (2011) confirmed that the basic phenomenon of hydrogen embrittlement is based on basic mechanism of hydrogen diffusion to, and concentration at, crack tips. This leads to the activation of hydrogen induced slip deformation. In addition, Hydrogen diffusion in austenitic stainless steels is strongly influenced by martensitic transformation and it is not influenced by strain in the absence of martensitic transformation as reported by T. Kanezaki, et al (2008).

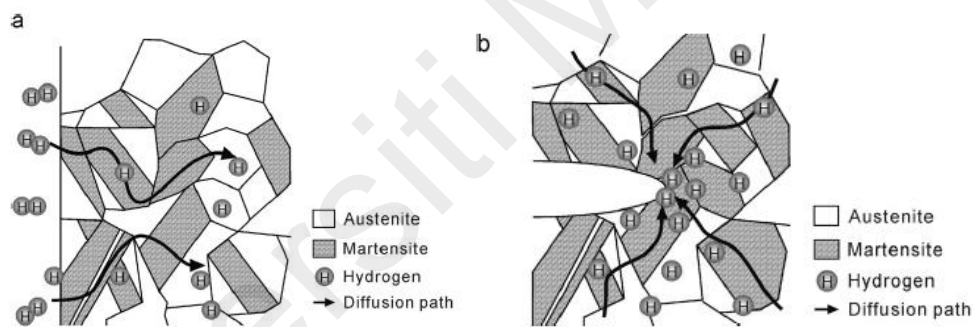


**Figure 2.2 : Schematic illustration of hydrogen diffusion path (a) from surface and (b) near crack tip. The transformed martensite acts as a highway for hydrogen diffusion in surrounding austenites (T. Kanezaki et. al, 2008)**

## 2.4 Hydrogen diffusion and solubility

Dissolved hydrogen in stainless steels increases dislocation mobility and slip planarity, resulting in plastic strain and stress concentrations that are heterogeneously distributed. In addition, nitrogen also increases dislocation mobility and localized plasticity whereas carbon

diminishes these properties as reported by Papula et al (2015). Internal stress that exists in a body that is stationary and in equilibrium with its surroundings is defined as residual stress. The elastic response of the material to an inhomogeneous distribution of nonelastic strains causes residual stresses. Residual stress is created in the material throughout all metal forming process. The amount of solved hydrogen in a metal is influenced by factors such as hydrogen diffusion and solubility.

The solved hydrogen content is additionally influenced by factors such as hydrogen pressure, temperature, microstructure, and material composition. It is generally up to a few ppm in ambient temperature and pressure condition (DeLuccia, J., 1988). Interstitially, hydrogen dissolves in metals by occupying octahedral and/or tetrahedral interstices. (Burke J. et. Al, 1972)

#### **2.4.1 Microstructural influence**

Film-like carbides are commonly found at prior austenite grain boundaries in tempered martensite, which are considered to be one of the most preferred places for excessive hydrogen trapping. A.W. Thompson, (1979). The hydrogen solubility of a metal is also affected by its structure; FCC iron has a higher hydrogen solubility than BCC iron.

As a result, during the martensite reaction, hydrogen rejection might occur, resulting in cracking and flaking. At ambient temperature, hydrogen's solid solubility in steel is relatively low, and most hydrogen is confined in dislocations, grain boundaries, inclusions, voids, interfaces, or impurity atoms. (Nagumo M. et. al, 2003)

## 2.5 Delayed Cracking

Delayed cracking is a stress-driven, time-dependent hydrogen redistribution phenomenon. It occurs when a steel component with previously created flaws is charged with hydrogen and subjected to a sub-critical stress. After procedures such as deep drawing, delayed cracking can occur in metastable austenitic stainless steels. It could take hours, days, or even weeks, for cracks to occur. Internal hydrogen, strain-induced  $\alpha'$ -martensite, and tensile residual stresses all contribute to delayed cracking. Papula.S , et. al. (2015), reported that Austenitic stainless steel 304 did not suffer from delayed cracking after deep drawing in its as-produced state with 3 ppm hydrogen. Presence of  $\alpha'$ -martensite reduces the resistance of austenitic stainless steels towards delayed cracking by increasing residual stresses in a formed material, enhancing the hydrogen diffusion and inherent high sensitivity to hydrogen embrittlement.

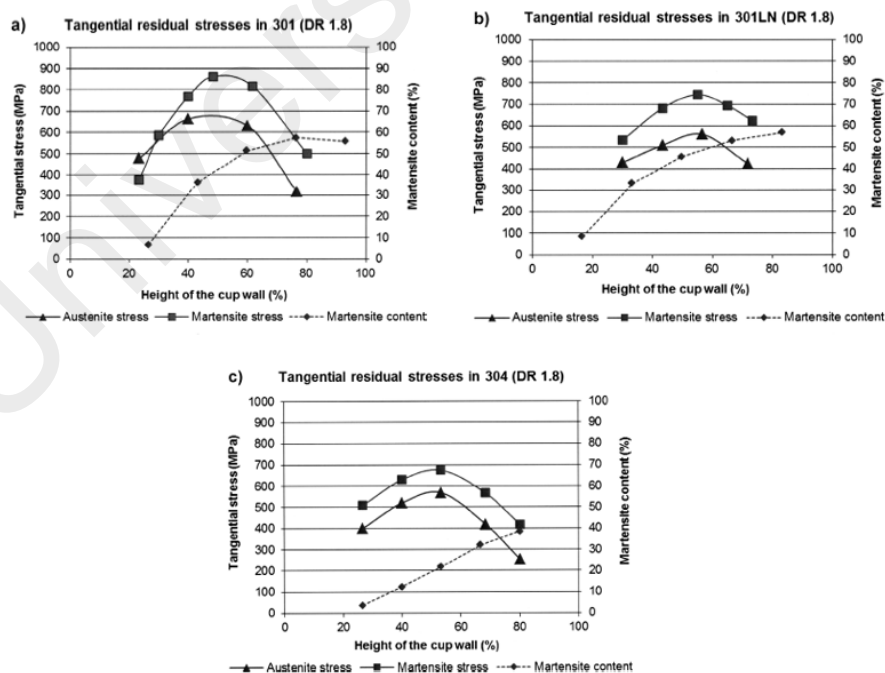


Figure 2.3 : Tangential residual stresses in  $\alpha'$ -martensite and austenite, Papula.S , et al (2015),

Tan CJ et al, (2019) reported that by using BHF roughly 3.6 to 3.9 times higher than the minimum force required to suppress wrinkles with 2 wt percent SiO<sub>2</sub> nano lubricant. The deep drawn SUS304L cups delayed cracks was effectively eliminated. With an increase in BHF, the time it took for the first fracture to form increases considerably. Within the same BHF range, the number of fractures for 2 wt% SiO<sub>2</sub> was lower than for 1 wt% and 3 wt% SiO<sub>2</sub>.

## **2.6 Effect of residual stress**

Residual stress has a major influence towards delayed cracking. (Yuying et al., 1992). It is an internal stress that persists in a body that is in equilibrium with its environment, in addition to elastic reaction of the material to an inhomogeneous distribution of nonelastic strains also causes residual stresses. It is also created in the material throughout all metal forming process.

Phase transformations also produce residual stresses to metallic materials. Due to the restraining impact of the stronger phases on the weaker ones, plastic strains are inhomogeneously distributed amongst the phases. Inhomogeneous plastic strain levels at different regions of the product cause residual stresses, which are the result of interactions between deformation, temperature, and microstructure (Wang Z. et. al., 2002).

Martensitic transition happens in metastable austenitic stainless steels as a consequence of plastic deformation, in which austenite is partially converted to thermodynamically more stable  $\alpha'$ -martensite. Local strain fields are generated by the strain-induced martensitic transformation, which results in varying internal stresses in both the austenite and  $\alpha'$ -martensite phases (Withers, P. J et. al 2001). In addition, a variation in strength between co-existing phases in the material, die/mold design or limitations from the gripping force on the workpiece, or temperature

gradients may all contribute to differences in real strain levels in various regions. (Wang Z. et. al., 2002)

Tan & Aslian (2019) reported that the valley points of the drawn cups have a higher risk of delayed cracks due to a significant concentration of residual stress. During the tool separation stage, the simulation results show a large rise in compressive to tensile stress at the valley points, as shown in Figure 2.4. The stress at the valley point grows dramatically after the tools separate from the deep drawn cup. Compressive stress tends to turn into tensile stress of a large magnitude. After the tools are detached from the deep drawn cup, there is a substantial increase in hoop stress, which leaves the valley points at a higher risk of delayed crack.

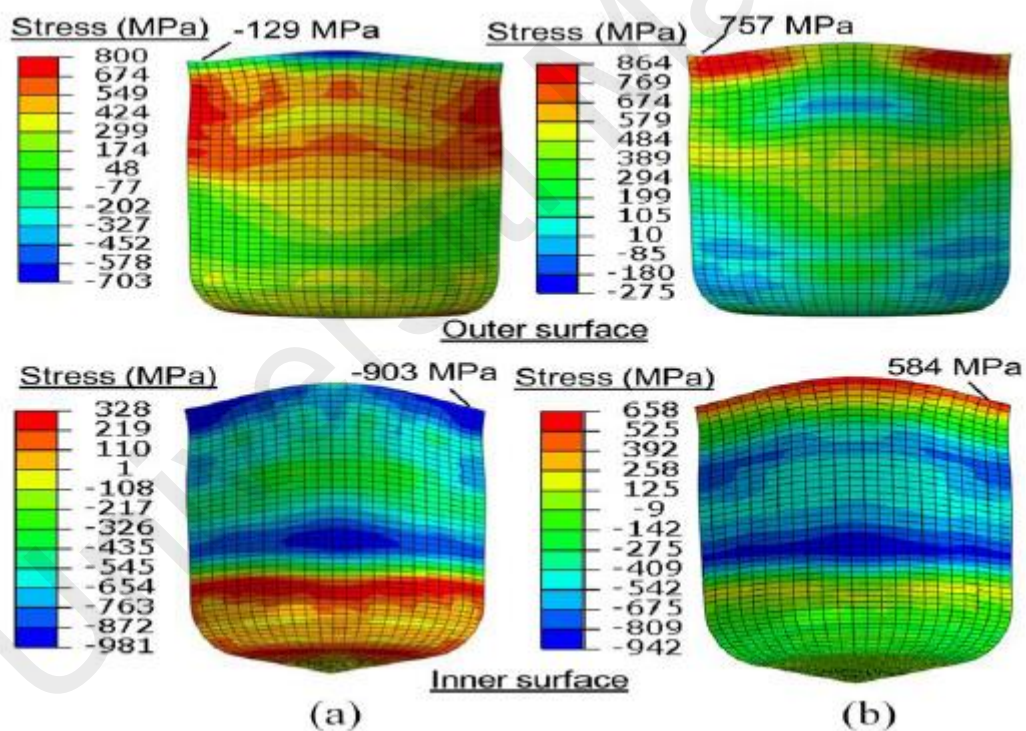


**Figure 2.4 : Hoop stress distribution at inner and outer surfaces of the cup at end of drawing stages (a) and tool separation stages (b) (Tan & Aslian , 2019)**

## 2.7 Strain induced $\alpha'$ -martensitic transformation

Various factors can influence the strain-induced  $\alpha'$ -martensitic transition, including the chemical composition of the steel, where Nickel, Chromium, Carbon, and Nitrogen play a significant role as reported by Berrahmoune et. al (2006). The volume fraction of strain-induced  $\alpha'$ -martensite as well as its characteristics are affected by alloying. Carbon and nitrogen, in particular, increase the hardness and brittleness of  $\alpha'$ -martensite, and so does a low nickel content is said to bear the same effect. In addition, they also reported that as the concentration of the strain induced martensite increases, the chances of for delayed crack to occurs also increase.

The strain-induced  $\alpha'$ -martensitic transition is almost constantly present during typical manufacturing operations such as cold rolling, deep drawing, wire drawing, grinding, or polishing, even though the starting temperature of martensite in commercial alloys is well below room temperature. Because stainless steels with metastable austenite have a tendency to change into martensite when cold worked, such as deep drawing, austenitic phase stability is critical as reported by Michler (2015). In addition, Papula et al (2015) reported that the presence of  $\alpha'$ -martensite is highly linked to the delayed cracking that occurs in austenitic stainless steels deep drawn cup with internal hydrogen concentrations of 5ppm or less.

## CHAPTER 3: METHODOLOGY

### 3.1 Introduction

This chapter will describe the methodology of the project for the hydrogen charging and deep drawn process for the SUS 304L blanks. The SUS 304L sheets of 1.17 mm thickness were procured locally from Bahru Stainless and are laser cut into a  $\varnothing 72$  mm diameter blank. The chemical composition of the SUS 304L steel are as shown in table 3-1.

**Table 3-1 : Chemical composition of SUS 304L blanks (wt%)**

C	S	P	Mn	Si	Cr	Ni	N
0.030	0.030	0.045	2.00	0.75	19.50	10.50	0.10

**Table 3-2 : Chemical composition of SUS 304 blanks (wt%)**

C	S	P	Mn	Si	Cr	Ni	N
0.068	0.007	0.025	0.97	0.52	18.7	8.07	0.029

In comparison between SUS 304 and SUS304L, SUS 304L contains less carbon content than SUS304, as shown by table 3.2 It has a low carbon content, which makes it resistant to intergranular corrosion, and a high nickel concentration, which makes it corrosion resistant. In addition, SUS304L is easy to process because it does not become excessively hard compared to SUS304.

The SUS 304L blanks are then will be hydrogen charged by replicating the same method for hydrogen charge as experiment conducted by Sang P.L et al (2015)., it is expected that the hydrogen content of the SUS304L blanks will be approximately equal.

In general, the whole process can be simplified into 5 main stages which is:

- I. Preparation of SUS 304L blanks
- II. Preparation of electrolytic & arsenic solution for electrolysis
- III. Hydrogen charging of SUS 304L Blanks / Cups by electrolysis
- IV. Deep drawing of hydrogen charged SUS 304L Blanks
- V. Sample evaluation

### 3.2 Experimental Flow Chart

The methodology adopted in this research work can be summarized in the flow chart shown in Figure 3.1 below.

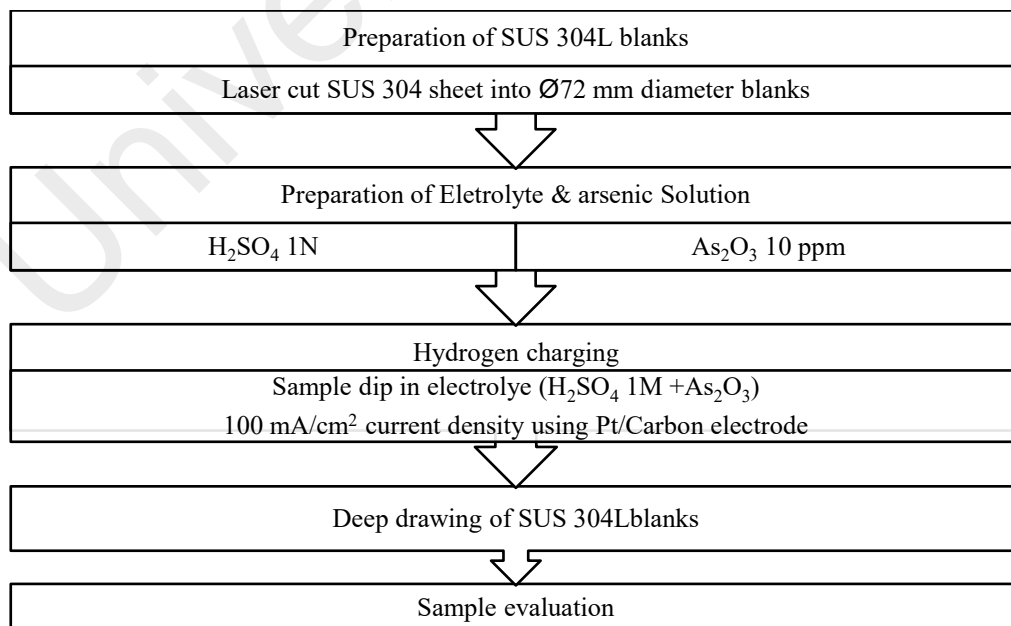


**Figure 3.1 : Experimental flow chart**

### 3.3 Preparation of electrolytic & arsenic solution

The chemicals used in the preparation of the electrolytes are:

- I. Sulphuric Acid (95-98%) which will then diluted into 1N of H<sub>2</sub>SO<sub>4</sub> solution
- II. Arsenic (III) Oxide, As<sub>2</sub>O<sub>3</sub> as hydrogen recombination poison
- III. Sodium Hydroxide, (10%), to dissolve arsenic for standard solution preparation

The concentrated sulphuric acid was diluted by using the dilution formula:

$$M_1V_1 = M_2V_2 \quad (1)$$

Where M<sub>1</sub> and V<sub>1</sub> is the initial Molarity and volume in litres of the concentrated H<sub>2</sub>SO<sub>4</sub>, and M<sub>2</sub> and V<sub>2</sub> is the final Molarity and volume of the desired stock solution of the electrolyte, where M<sub>2</sub> is 1N (0.5 M) and V<sub>2</sub> is 1 litre for every stock of solution per batch.

The 10 ppm As<sub>2</sub>O<sub>3</sub> solution was prepared by dissolving the As<sub>2</sub>O<sub>3</sub> powder in 10% on NaOH, and it is then neutralised with 1N of H<sub>2</sub>SO<sub>4</sub> in excess. Final volume of stock solution of 1 litre was prepared by adding 1 litres of distilled water.

### 3.4 Hydrogen charging

A solution of 1N H<sub>2</sub>SO<sub>4</sub> was used to electrochemically introduce hydrogen into the samples. The electrolyte was poisoned with 10 mg/L As<sub>2</sub>O<sub>3</sub> to avoid hydrogen recombination. The constant supply of electrical power for charging are maintained by using a standard voltage controller, and the current densities are kept constant at 100 mA/cm<sup>2</sup>. One platinum mesh served as the anode, while the sample served as the cathode as shown in figure 3.2 with

charging durations of 6, 12, and 24 hours were chosen. Prior to charging and after charging, the samples are cleaned with cleaning alcohol and then air dried.

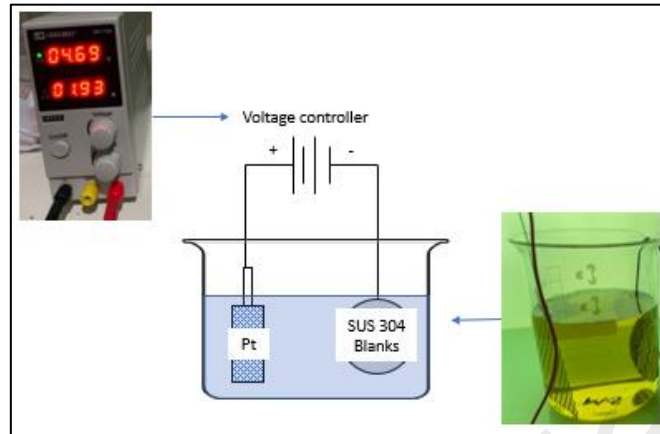


**Figure 3.2 : Setup for the hydrogen charging of the SUS 304L blanks**

The current density was determined by calculating mean surface area of the sample and Pt-mesh. The needed current to achieve the required current density are then determined by multiplying the current density  $I_{CD}$  with the mean surface area, as shown in equation 2 below.

$$I = I_{CD} \times S \quad (2)$$

Where  $I$  is the current, mA,  $I_{CD}$  is the current density, mA/cm<sup>2</sup> and  $S$  = the surface area of the electrode (mean cross-sectional area of the solution), cm<sup>2</sup>

### 3.5 Deep Drawing

The deep drawing under blank holding force was conducted using a hydraulic press setup with a SKD-11 tool steel die, mold and a load sensor, as per shown in figure 3.3. As reported previously by study conducted by Tan CJ et al (2019), the TiN coated die have a slightly smoother surface roughness compared to the uncoated die which is 0.382  $\mu\text{m}$  and 0.581  $\mu\text{m}$  respectively as shown in figure 3.4 & 3.5. The surface roughness of the dies is measured using

Mitutoyo SJ-210 Roughness Tester which are tuned to work according to ISO1997. The SUS 304L blanks was laser cut into with diameter of  $\varnothing 72$  and 1.17 mm thickness. The edges of the laser cut blanks were polished to remove any uneven edges due to the lase cut prior to the deep drawing BHF.



**Figure 3.3 : (a) TiN Coated Die (b) Uncoated Die (Tan CJ et. al 2019)**

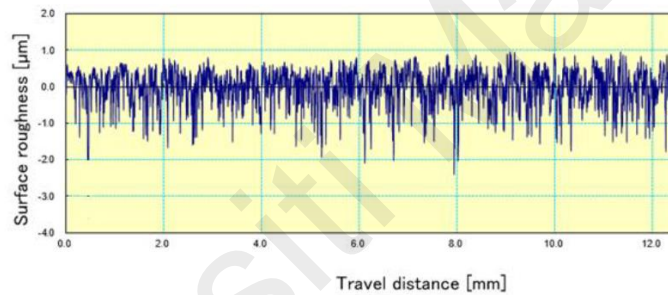


**Figure 3.4 : Surface roughness profile of TiN coated die (Tan CJ et. al 2019)**

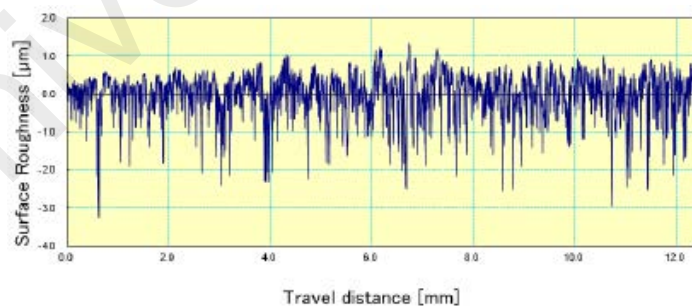


**Figure 3.5 : Surface roughness profile of finely polished SKD-11 tool steel uncoated die (Tan CJ et. al 2019)**

Prior to deep drawing, the die and the blank holder are polished using orbital handheld sander polisher with 4000 rpm speed. The polishing process starts with 800 and 1000 grit sandpaper and it is polished using a metallographic polishing pad that is paired with diamond

paste of 3 micron mixed with diamond lubricant. Ensuring the die and blanks smooth is essential to ensure that its surface roughness is in good condition for the drawing process.

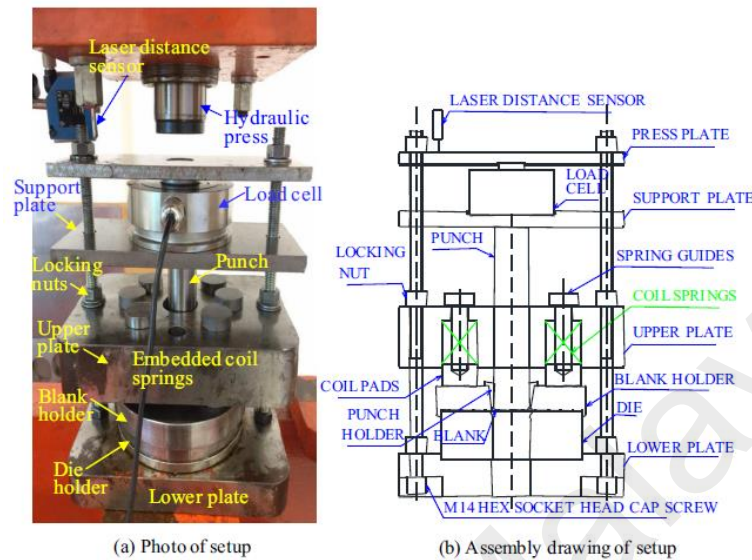


**Figure 3.6 : Setup for the Deep drawing process for blank holding force BHF (Tan CJ et. al 2019)**

The BHF was done with forces from 8,9,10 and 11 kN using uncoated die for the hydrogen charged samples. An additional hydrogen charged samples were also undergo BHF 7, 10, and 12 kN using uncoated die. At a constant speed of 1.1 mm/s, a 25-ton motorized hydraulic press compresses a circular blank into a completely drawn cylindrical cup. The blank holder is just under the drawing die.

The BHF acts on the blank when the top plate is compressed. During the drawing test, two locking nuts are utilized to prevent the coil spring from returning and to maintain a steady BHF value. Through a support plate, a 30-ton load cell is mounted on the top of the drawing punch. The press then compresses the load cell and the press plate, causing the punch to move into the die. A laser distance meter oriented vertically to the press plate measures the punch's travel distance.

## CHAPTER 4: RESULTS & DISCUSSION

### 4.1 Hydrogen Charging

Hydrogen charging was conducted as described in chapter 3. It was observed that the hydrogen charged samples will become darker after it is hydrogen charged for all duration of 6, 12 and 24 hours respectively, as the comparison shown in figure 4.1. During the charging, the presence of air bubbles is observed onto the surface of the charged samples. As the electrolytes is a combination of  $\text{H}_2\text{SO}_4$  and  $\text{As}_2\text{O}_3$ ,  $\text{SO}_4^{2-}$  ions will react with the electrons, as electrical current is applied. At the anode (SUS 304L blanks),  $\text{SO}_2$  and  $\text{O}_2$  gas will be produced, while at the cathode (inert electrode)  $\text{H}_2$  gas is produced.

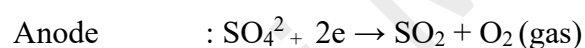


**Figure 4.1 : Non hydrogen charged blanks (left), Hydrogen charged blanks (right)**

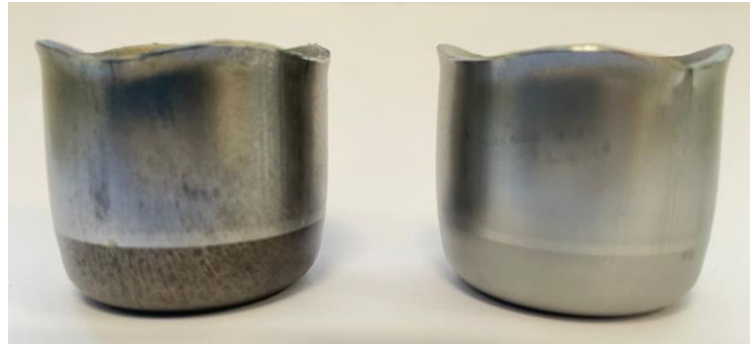


**Figure 4.2 : Hydrogen charged SUS304L cup (left) Non hydrogen charged cups (right)**

#### **4.2 Deep drawing at elevated BHF**

The blank holding force was done at 8,9,10 and 11kN on the uncoated die while the 7,10 and 12 kN with TiN coated die. Based on all of the samples that has been produced, it was found that there's a clear-cut difference between HC sample before BHF and vice versa. The sample that has undergo deep drawing BHF prior to hydrogen charging showed an increasing trend for the number of cracks. As the duration of charging increases from 6 to 12 and 24 hours, it was observed that the number of cracks also increased. However, the samples that was hydrogen charged prior to deep drawing BHF showed almost no change in trends, despite all of the sample also have cracks after deep drawing.



**Figure 4.3 : Samples charged for 24 hours after deep drawn**

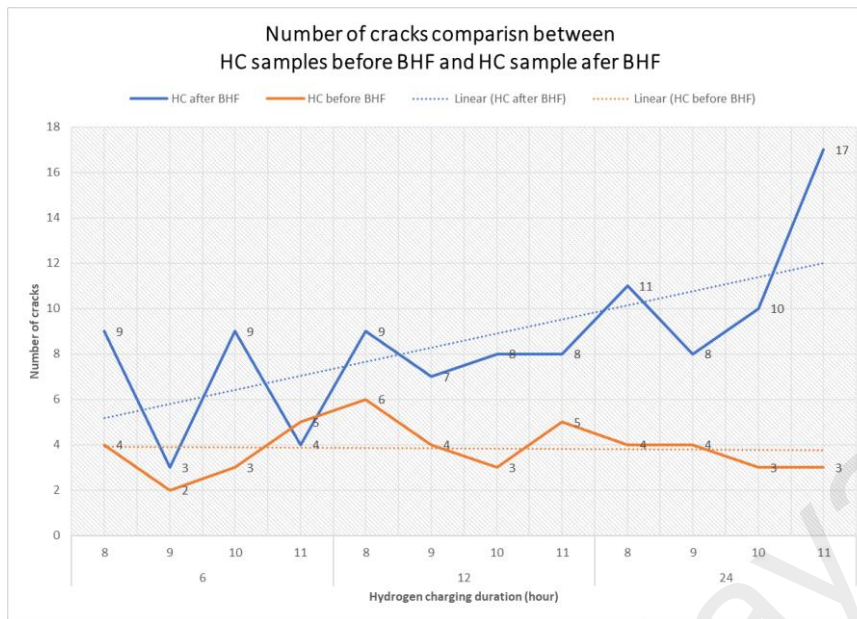


**Figure 4.4 : Number of cracks comparison for HC sample before BHF and vice versa**

The crack length also showed a clear difference between the two groups of samples. Samples that have undergone deep drawing BHF prior to HC possess a much more longer crack length in average of about more than 15 mm whereas in comparison, the HC charged blanks prior to deep drawing BHF showed a crack that is only less than 10 mm in length as shown in figure 4.5 and 4.6 respectively. This phenomenon is highly correlated with the residual stress, as the samples that is charged after deep drawing is already under immense residual stress. As stated by previous study by Tan and Aslian (2019), the tip of the formed cups is the area that is most prone to cracks as the stress is mostly concentrated there after the deep drawing is completed as show in one of the sample photos in figure 4.3. The hydrogen charging will initiate the hydrogen attack toward the microstructure of the steel, which will indefinitely accelerate and produces much more cracks.

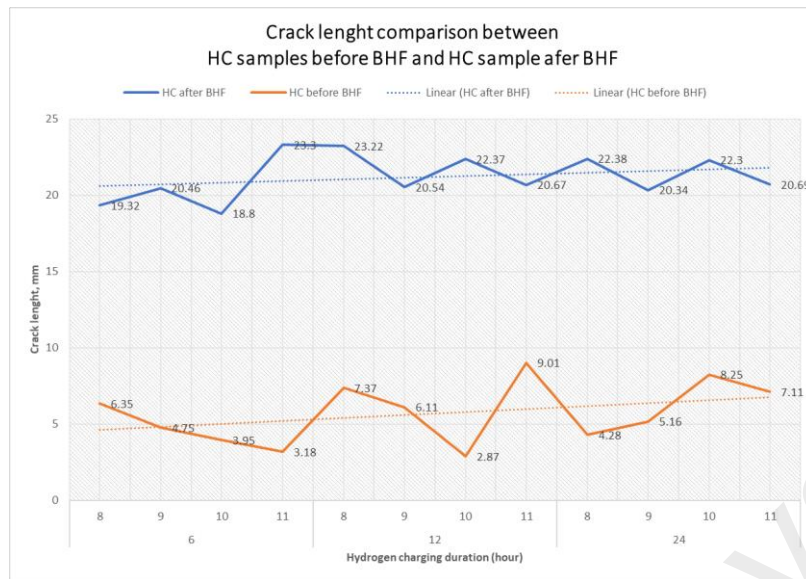


**Figure 4.5 : Crack length comparison for HC sample before BHF and HC after BHF**

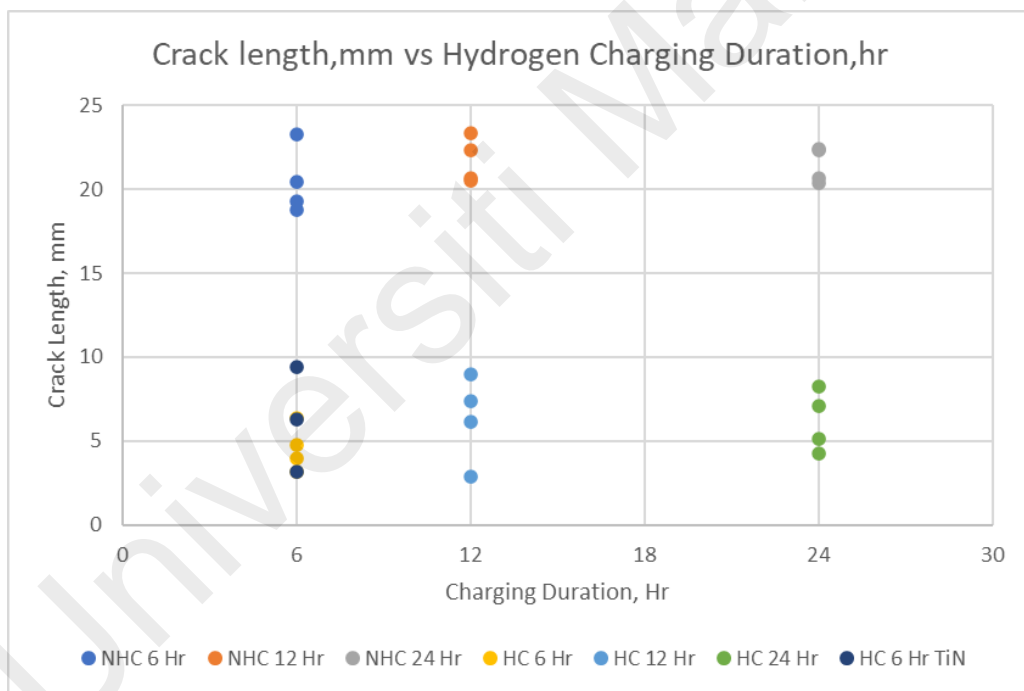


**Figure 4.6 : Crack length comparison for HC sample before BHF and HC after BHF**

By changing the die to TiN coated die, it was expected that under the tested BHF range, no cracks should have formed. However, delayed cracks still appear after 6 hours despite that the BHF was done within a safe BHF range for successful drawn cups (Tan CJ, et al. 2019) as the SUS304L blanks was charged for 6 hours prior to deep drawing. However, the severity of the

cracks of the cups that was drawn using TiN coated die, were deemed to be much less than the on using uncoated die. The crack length in general was almost the same as with the drawn cups using the uncoated die. However, the duration for the crack to formed showed to be much slower compared to the cups that is drawn by the uncoated die. Thus, the hydrogen charging duration influence speed of the crack appearance for the first 1 hour as stated in table 4.1. Overall, the sample group that undergo deep drawing BHF prior to HC shows a slightly faster rate compared to the other group.

**Table 4-1 : Number of crack and crack lengths for HC after BHF, (HCAB), HC before BHF, (HCBB) and HC before BHF with TiN die, (HCBB-TiN) samples**

	Sample	Die (Un-coated / TiN Coated)	Blank holding Forces, BHF (kN)	Hydrogen Charging duration (hours)	Number of crack after 1st hour	Number of crack after 6 hour	Crack length (mm)
HC after BHF (HCAB)	HCAB 8-6	Uncoated Die	8	6	1	9	19.32
	HCAB 9-6		9		2	3	20.46
	HCAB 10-6		10		3	9	18.8
	HCAB 11-6		11		2	4	23.3
	HCAB 8-12		8	12	3	9	23.22
	HCAB 9-12		9		3	7	20.54
	HCAB 10-12		10		2	8	22.37
	HCAB 11-12		11		3	8	20.67
	HCAB 8-24		8	24	6	11	22.38
	HCAB 9-24		9		5	8	20.34
	HCAB 10-24		10		5	10	22.3
	HCAB 11-24		11		7	17	20.69
	HCBB 8-6		8		Uncoated Die	6	0
HCBB 9-6	9	0	2	4.75			
HCBB 10-6	10	1	3	3.95			
HCBB 11-6	11	1	5	3.18			
HCBB 8-12	8	12	1	6		7.37	
HCBB 9-12	9		1	4		6.11	
HCBB 10-12	10		1	3		2.87	
HCBB 11-12	11		2	5		9.01	
HCBB 8-24	8	24	1	4		4.28	
HCBB 9-24	9		1	4		5.16	
HCBB 10-24	10		1	3		8.25	
HCBB 11-24	11		1	3		7.11	
HCBB-TiN7-6	7		TiN Coated die	6		0	2
HCBB-TiN10-6	10	0			6	3.13	
HCBB-TiN12-6	12	0			5	9.42	

The maximum drawing load for the group of samples was also observed. The trend shows that for the SUS304L blanks that was charged prior to deep drawing shows an increasing trend on the drawing load as shown in figure 4.8. As the charging duration was increased from 6 to 24 hours, the peak forming load varies from 108 kN to 117kN in an increasing manner. In

comparison with the SUS304L that was charged after deep drawing, the trend of the peak load shows almost no change as shown in figure 4.8, which is true as the blanks are actually not charged during the deep drawing, but it was hydrogen charged after it is deep drawn into cups.

In addition, as shown in figure 4.7, for the same charging duration of 6-hour, deep drawing using TiN coated die shows higher range for forming load from 118 kN to 123 kN, whereas for the uncoated die is between 109 kN to 111.9 kN for the same hydrogen charging of 6 hours. It also shows that as the charging duration increases to 12 and 24 hours, the peak forming load also increases linearly. Longer charging duration caused the surface of the blanks to become more harder as it requires more energy to cause deformation towards the blanks to become drawn into cups.

The forming load for the samples that was hydrogen charged and deep drawn was also observed as shown in figure 4.7,4.8,4.9,4.10 and 4.11. Samples that used the TiN coated die, shows the highest peak forming load, which reaches more than 123 kN, for all 3 deep drawing process that is done at 7,10 and 12 kN respectively with an average load of 120 kN. In comparison to the charged and uncharged samples that is deep drawn using uncoated die, the peak load did not exceed 120 kN, but in average the peak load is only about 112 kN. This shows that the hydrogen charging has caused a resistance on the surface. This result is due to the difference in surface roughness of the coated and uncoated die as reported by Tan et. al (2021) whereby the coated die has smoother surface roughness of 0.382  $\mu\text{m}$  and compared to uncoated die that has 0.581  $\mu\text{m}$ , thus results in the difference in the peak load performance of the samples during deep drawing process using different dies.

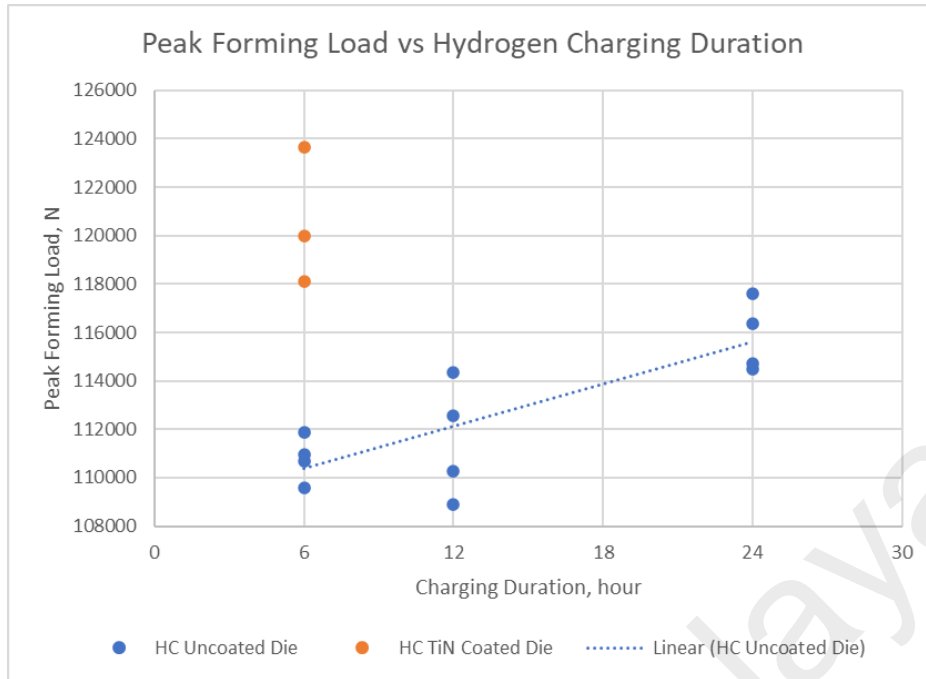


**Figure 4.7 : Peak Forming Load vs HC duration**

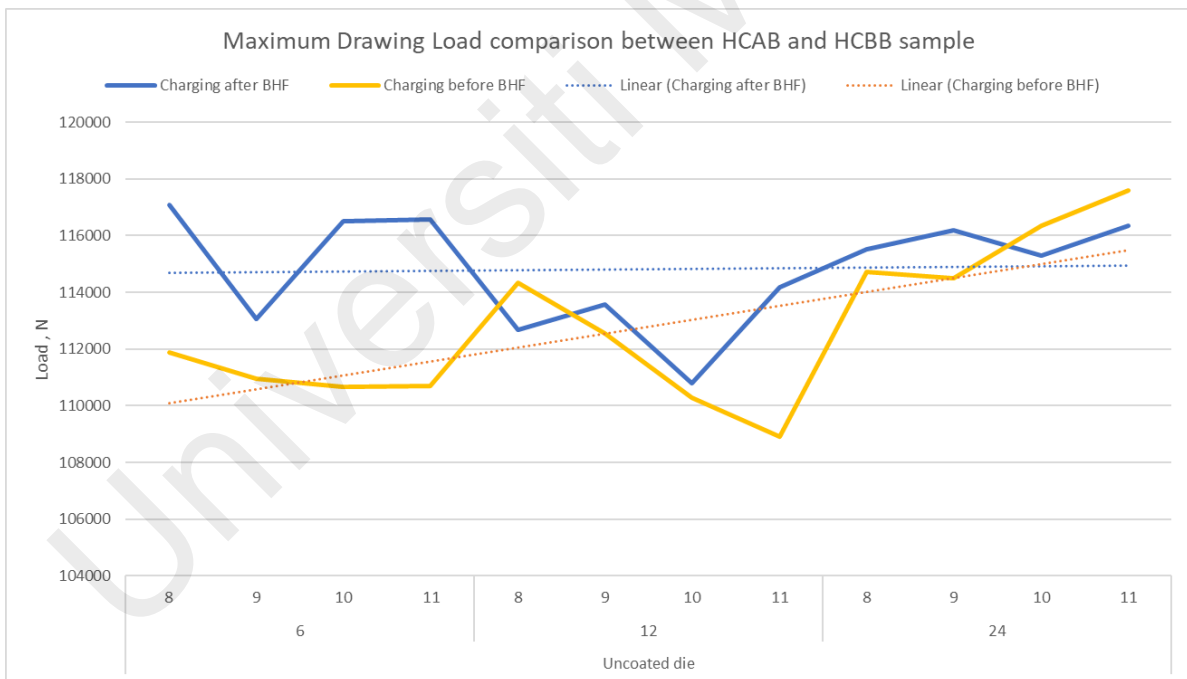


**Figure 4.8 : Maximum drawing load comparison between HC after deep drawing samples and HC before deep drawing**

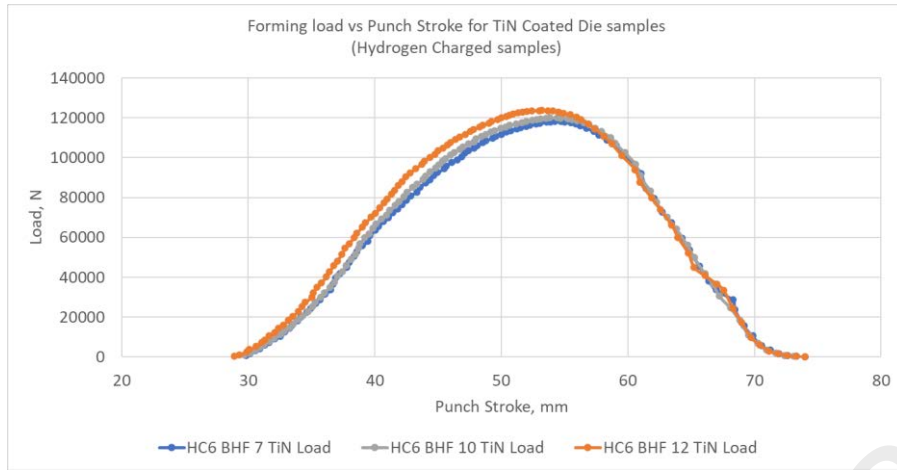


**Figure 4.9 : Forming load vs punch stroke for TiN Coated die samples hydrogen charged for 6 hours**

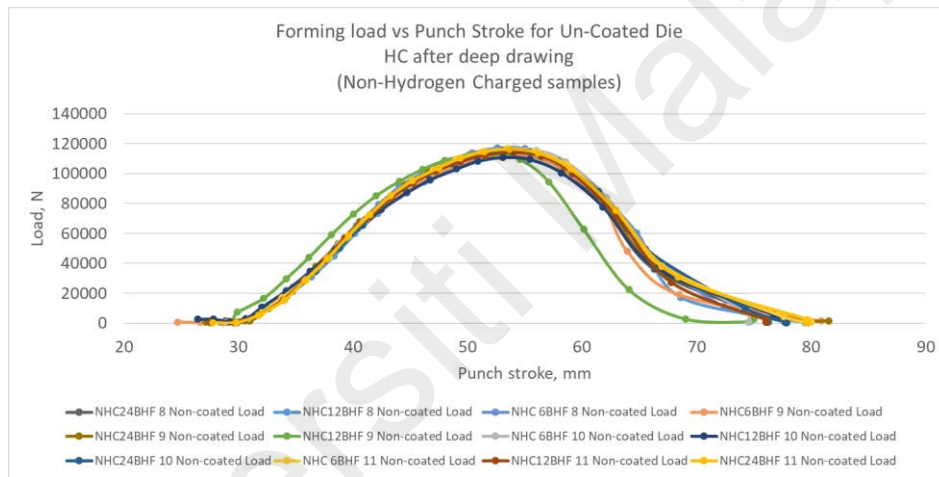


**Figure 4.10 : Forming load vs punch stroke for un-coated die HC after deep drawing**

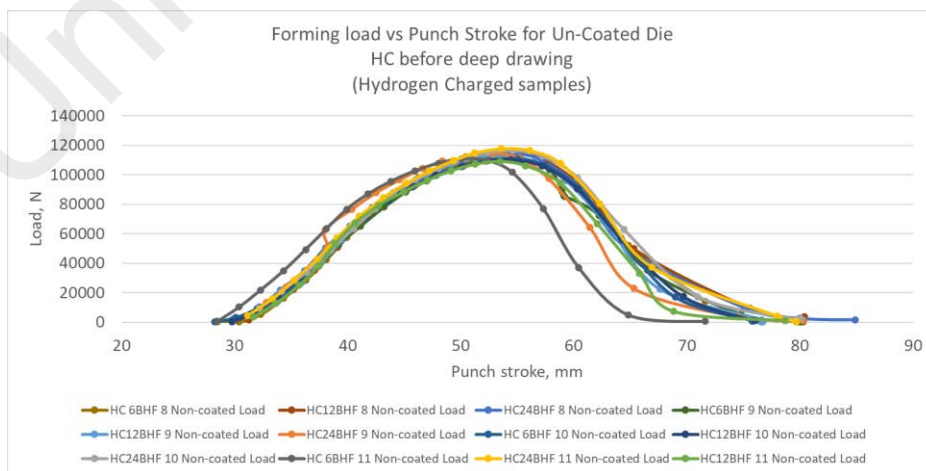


**Figure 4.11 : Forming load vs Punch stroke for un-coated die HC before deep drawing**

## CHAPTER 5: CONCLUSION

### 5.1 Summary

All cups formed with uncoated die shows a crack appearance. SUS 304L cups that is hydrogen charged prior to applying BHF between 8-11 kN shows a less severe effect of delayed crack. The number of cracks & the length of cracks showed a linear increase as the charging duration is increased from 6, 12 to 24 hours. In addition, charging the blanks after deep drawing process shows a significant effect to towards the severity of the cracks formed. Hydrogen charging prior to deep drawing shows less severe cracks, despite there are cracks formed for all of the samples that is hydrogen charged, regardless of the BHF applied. In addition, SUS 304L cups that undergo BHF first and hydrogen charged afterwards, shows an accelerated delayed crack appearance within less than 6 hours. A higher BHF applied to the blanks and undergo hydrogen charging, shows a faster appearance for delayed cracks within the first 1-6 hour. Longer duration of hydrogen charging will produce a more severe & longer cracks for all BHF samples. Hydrogen charged blanks that undergo BHF at 7, 10 and 12 using coated die also showed a crack formation after 6 hours. Despite crack-free cups were expected to formed from the non-HC blanks with TiN coated die for the entire successful BHF drawing range based on previous study, crack was still formed on cups due to the hydrogen charging process.

### 5.2 Recommendations for Future Project

- I. Consider the other parameter that influences the hydrogen absorption such as higher temperature and higher pressure

- II. Investigate the most suitable parameter of BHF and die to prevent the delayed cracks from appearing for the hydrogen charged samples
- III. Charging should be done with a magnetic stirrer, in order to ensure that the electrolyte mixture with the poison is evenly distributed

Universiti Malaya

## REFERENCES

- Sang, P.L., Seung, K.H., Jin, K.L., In, S.S., Dong, S.B. (2015). Effect of Hydrogen Charging on the Mechanical Properties of 304L Stainless Steels. *Journal of the Korean Society for Power System Engineering*, 19(5),73-79. <http://dx.doi.org/10.9726/kspse.2015.19.5.073>
- Kanezaki T., Narazaki C., Mine Y., Matusuoka S., Murakami Y., (2008). Effects of hydrogen on fatigue crack growth behavior of austenitic stainless steels. *International Journal of Hydrogen Energy*, 33, 2604-2619. <https://doi.org/10.1016/j.ijhydene.2008.02.067>
- Murakami Y., Matsuoka S., Olive J.M., Awane T., Saintier N., (2011). Analyses of hydrogen distribution around fatigue crack on type 304L stainless steel using secondary ion mass spectrometry. *International Journal of Hydrogen Energy*, 36, 8630-8640. <https://doi.org/10.1016/j.ijhydene.2011.03.111>
- Benson J.R., Dann R.K., Roberts J.L., (1968) Hydrogen embrittlement of stainless steel. *Transactions of the Metallurgical Society of AIME* 242, 2199
- Bentley, A.P., Smith, G.C., (1986) Phase transformation of austenitic stainless steels as a result of cathodic hydrogen charging. *Metallurgical Transactions A17*, 1593–1600 <https://doi.org/10.1007/BF02650096>
- DeLuccia, J. (1988). Electrochemical aspects of hydrogen in metals. In *Hydrogen embrittlement: prevention and control*. ASTM International.
- Burke, J., M. L. Mehta, and R. Narayan (1972). Hydrogen embrittlement of type 304LL austenitic stainless steel. *Cong. L'Hydrogene dans les Metaux*, 1, 149-158

- De Luccia J.J., Agarwala V. S., (1978) Effects of magnetic field on hydrogen evolution reaction and its diffusion in iron and steel, Proc of 7th Int. Cong on Metallic Corrosion, Hotel Nacional/Rio de Janeiro, Brasil, October, (1978), 795-805
- Yuying, Y., Chunfeng, L. and Hongzhi, X., (1992). Study of longitudinal cracking and the forming technology for deep-drawn austenitic stainless steel cups, Journal of Materials Processing Technology, 30, 167-172.
- Tan, C.J., Ibrahim, M.S. & Muhamad, M.R., (2019). Preventing delayed cracks in SUS304L deep drawn cups using extreme blank holding forces aided by nano lubrication, International Journal Advance Manufacturing Technology, 100, 1341–1354. <https://doi.org/10.1007/s00170-018-2772-5>
- Wang, Z. and Gong, B., (2002). Residual stress in the forming of materials, in: Handbook of residual stress and deformation of steel, ASM International, Materials Park, Ohio, 141-149
- Papula S., Saukkonen T., Talonen J., Hänninen H., (2015). Delayed Cracking of Metastable Austenitic Stainless Steels after Deep Drawing, ISIJ International, 55, 10, 2182-2188. <https://doi.org/10.2355/isijinternational.ISIJINT-2015-078>
- Thompson A.W., (1979). Effect of Metallurgical Variables on Environmental Fracture of Engineering Materials, Environment-Sensitive Fracture of Engineering Materials, Z.A. Forouli, ed., TMS-AIME, 379-410.
- Nagumo, M., Sekiguchi, S., Hayashi, H. and Takai, K., (2003) Enhanced susceptibility to delayed fracture in pre-fatigued martensitic steel, Materials Science and Engineering A, 344, 86-91. [https://doi.org/10.1016/S0921-5093\(02\)00403-3](https://doi.org/10.1016/S0921-5093(02)00403-3)

- Withers, P. J. and Bhadeshia, H. K. D. H., (2001) Residual stress, Part II – Nature and origins, *Materials Science and Technology*, 17, 366-375.  
<https://doi.org/10.1179/026708301101510087>
- Tan, C.J., Phoo Y.H.(2021). Eliminating Delayed Cracks in Deep-Drawn SUS304L Cups Under Wider Range and Lower Magnitude of Blank Holding Forces Using Tin Coated Die. <https://doi.org/10.21203/rs.3.rs-515980/v1>
- Tan, C. J., & Aslian, A. (2019). FE simulation study of deep drawing process of SUS304 cups having no delayed cracks under enhanced blank holding force. *Proceedings of the Institution of Mechanical Engineers, Part B: Journal of Engineering Manufacture*, 1–11. <https://doi.org/10.1177/0954405419855230>
- Bak, S., Abro, M., & Lee, D. (2016). Effect of Hydrogen and Strain-Induced Martensite on Mechanical Properties of AISI 304 Stainless Steel. *Metals*, 6(7), 169.  
<https://doi.org/10.3390/met6070169>
- Berrahmoune, M. R., Berveiller, S., Inal, K., & Patoor, E. (2006). Delayed cracking in 301LN austenitic steel after deep drawing: Martensitic transformation and residual stress analysis. *Materials Science and Engineering A*, 438–440(SPEC. ISS.), 262–266. <https://doi.org/10.1016/j.msea.2006.02.189>
- Michler, T. (2015). Austenitic Stainless Steels. *Reference Module in Materials Science and Materials Engineering*, (June 2015), 1–6. <https://doi.org/10.1016/b978-0-12-803581-8.02509-1>